Inorganic Chemistry

Article

pubs.acs.org/IC

# A Tetranitrosyl [4Fe−4S] Cluster Forms En Route to Roussin's Black Anion: Nitric Oxide Reactivity of $[Fe_4S_4(LS_3)L']^{2-}$

Eric Victor and Stephen J. Lippard*

Department of Chemistry, Massachusetts Institute of Technology, Cambridge, Massachusetts 02139, United States

Supporting Information

**ABSTRACT:** Previous studies provide evidence that [4Fe−4S] clusters serve as targets of reactive nitrogen oxide species in biology. The products of this reaction range from dinitrosyliron complexes, $[Fe(NO)_2L_2]^-$, to Roussin's black anion, $[Fe_4S_3(NO)_7]^-$. To date, the pathways by which these reactions occur have not been fully elucidated. In this study, we prepared the site-differentiated complexes $[Fe_4S_4(LS_3)L']^{2-}$ ($LS_3$ = 1,3,5-tris(4,6-dimethyl-3-mercaptophenylthio)-2,4,6-tris(*p*-tolylthio)benzene; L′ = Cl, SEt, SPh, $N_3$, 2-SPyr, Tp, $S_2CNEt_2$) to serve as synthetic models for biological [4Fe−4S] clusters and studied their reactivity toward NO(g) and $Ph_3CSNO$. The products were characterized by X-ray crystallography, mass spectrometry, and IR, electron paramagnetic resonance (EPR), and $^1H$ NMR spectroscopy. In all cases reported here, the reactions proceed via formation of the $S = {}^1/_2$ species $[Fe_4S_4(NO)_4]^-$, which ultimately converts to EPR-silent $[Fe_4S_3(NO)_7]^-$.

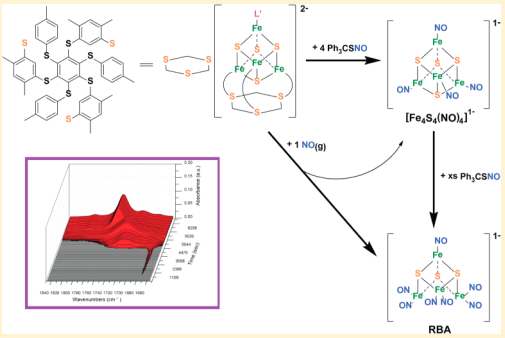


## INTRODUCTION

Following the initial discovery of nitric oxide (NO) as the endothelium-derived relaxation factor, NO has been implicated in many important biological functions including neurotransmission and the immune response.[1] NO is capable of influencing biological systems by forming *S*-nitrosothiols, *N*-nitrosamines, and metal nitrosyls.[2] The biochemistry of NO and reactive nitrogen oxide species (RNOS) includes interactions with metal-containing proteins.[2a,3] Iron−sulfur clusters react with NO to regulate intracellular iron levels, and the oxidative stress response involves degradation of the clusters to form protein-bound or low-molecular-weight dinitrosyliron complexes (DNICs; Figure 1).[4] These DNICs arise from degradation of [2Fe−2S] and [4Fe−4S] clusters and trigger protein conformational changes that facilitate the binding of these proteins to DNA and other cellular targets.[4b,5]

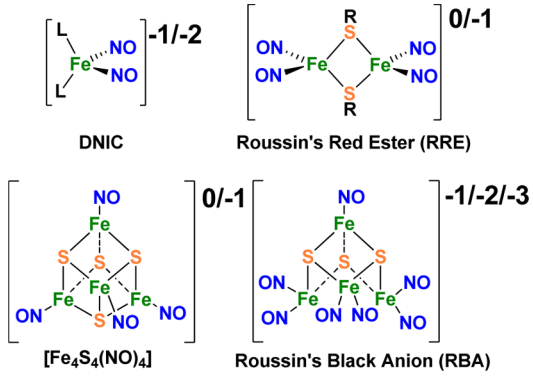


**Figure 1.** Iron−sulfur nitrosyl compounds.

The reactions between NO and iron−sulfur clusters have not been fully elucidated, however, particularly within biological settings.[5a,6] Initially, DNICs were considered to be the major product formed during nitrosation of protein-bound [4Fe−4S] clusters based on electron paramagnetic resonance (EPR) spectra that matched those of known species.[7] Degradation of the [4Fe−4S] active site in cytosolic aconitase by NO was implicated in the regulation of intracellular iron levels.[4,8] An apical iron atom is extruded from the core of these clusters to form [3Fe−4S] units and DNICs, as evidenced by their characteristic $g_{avg}$ = 2.03 rhombic EPR spectral features. The EPR technique is limited, however, for it can only detect paramagnetic species and does not provide unambiguous structural information. Work from our laboratory and others has demonstrated that the action of NO on protein-bound iron−sulfur clusters also generates EPR-silent species, which may, in some cases, be the major nitrosated product.[5a,b,9] In one study using recombinant *Pyrococcus furiosus* ferredoxin (D14C mutant), the EPR-silent Roussin's black anion (RBA), $[Fe_4S_3(NO)_7]^-$, was detected as the major product by nuclear resonance vibrational spectroscopy (NRVS).[9a] Recently, the [4Fe−4S] clusters of Wbl proteins, which are implicated in the induction of sporulation in *Streptomyces* and virulence gene expression in mycobacteria, were shown to form 2 equiv of Roussin's red ester (RRE) having the chemical formula $[Fe_2(\mu\text{-}SR)_2(NO)_4]$.[5a,b]

To gain further insight into the nature of the reactions of NO and other RNOS with iron−sulfur clusters, we have studied this chemistry using small-molecule analogues of the metalloprotein

**Received:** March 13, 2014
**Published:** April 28, 2014

   dx.doi.org/10.1021/ic500586g | *Inorg. Chem.* 2014, 53, 5311−5320

**Scheme 1. Reactivity Pathways of Synthetic [4Fe−4S] Clusters with NO(g) and $Ph_3CSNO$**

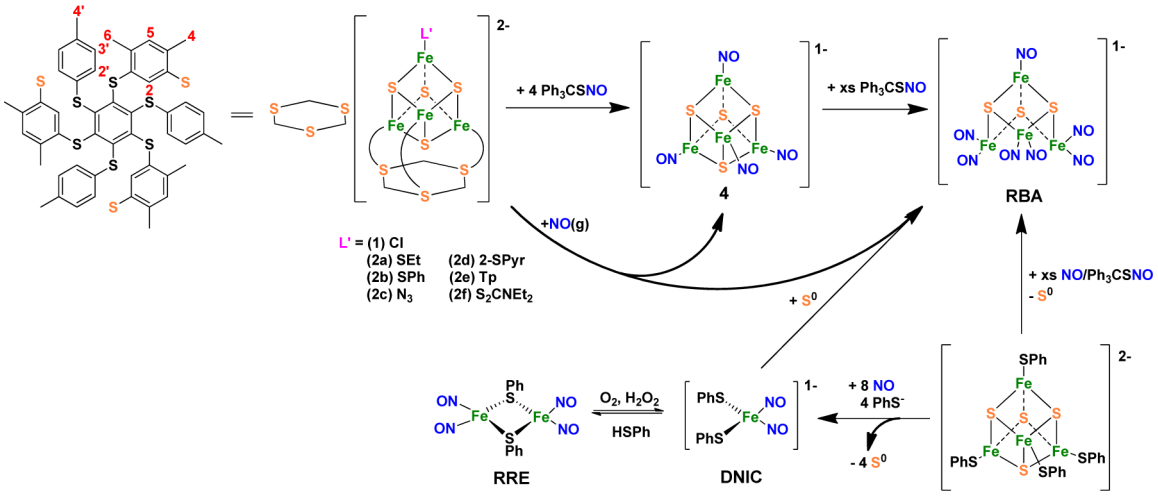


**Table 1. X-ray Crystallographic Data for 2c·4MeCN·$Et_2O$·0.5$H_2O$, 2f·2.5$Et_2O$, and $(Cp^*_2Fe)$4 at 100 K**

| | 2c·4MeCN·$Et_2O$·0.5$H_2O$ | 2f·2.5$Et_2O$ | $(Cp^*_2Fe)$4 |
|---|---|---|---|
| formula | $C_{113}H_{110}Fe_4N_8O_{1.50}P_2S_{13}$ | $C_{114}H_{120}Fe_4NO_{2.5}P_2S_{15}$ | $C_{20}H_{30}Fe_5N_4O_4S_4$ |
| formula weight | 2306.21 | 2310.35 | 797.7 |
| cryst syst | triclinic | triclinic | triclinic |
| space group | $P\bar{1}$ | $P\bar{1}$ | $P\bar{1}$ |
| *a*, Å | 15.1180(12) | 14.2454(10) | 11.8500(9) |
| *b*, Å | 16.8098(13) | 16.7845(11) | 14.8878(11) |
| *c*, Å | 22.7156(18) | 26.5044(18) | 17.1595(13) |
| *α*, deg | 96.5660(10) | 87.4210(10) | 90.1420(10) |
| *β*, deg | 105.1310(10) | 76.7280(10) | 105.8060(10) |
| *γ*, deg | 91.6890(1) | 69.4440(10) | 92.2720(10) |
| *V*, Å$^3$ | 5525.4(8) | 5770.3(7) | 2910.3(4) |
| *Z* | 2 | 2 | 4 |
| $\rho_{calcd}$, g/cm$^3$ | 1.386 | 1.330 | 1.821 |
| $\mu$, mm$^{-1}$ | 0.842 | 0.840 | 2.754 |
| *θ* range, deg | 1.80−25.31 | 1.49−27.33 | 1.37−25.03 |
| completeness to *θ*, % | 99.2 | 99.4 | 100.0 |
| reflns collected | 89 482 | 108 120 | 45 631 |
| indep reflns | 19 989 | 25 908 | 10 269 |
| *R*(int) | 0.1308 | 0.0505 | 0.0741 |
| restraints | 30 | 30 | 0 |
| parameters | 1295 | 1281 | 690 |
| max, min transmission | 0.7452, 0.6104 | 0.7455, 0.6570 | 0.7452, 0.6438 |
| R1 (wR2) [$I > 2\sigma(I)$] | 0.0698 (0.1338) | 0.0537 (0.1485) | 0.0419 (0.0631) |
| R1 (wR2) | 0.1353 (0.1569) | 0.0808 (0.1643) | 0.0829 (0.0722) |
| GoF($F^2$) | 1.035 | 1.264 | 1.008 |
| max, min peaks, e/Å$^3$ | 1.150, −1.020 | 2.322, −0.741 | 0.550, −0.442 |

active sites. Direct reaction of $[Fe_4S_4(SPh)_4]^{2-}$ with NO(g) or $Ph_3CSNO$ results in formation of RBA and, in the presence of additional thiolates, DNICs.[6a,10] In the present study, we extend these investigations to previously reported, site-differentiated $[Fe_4S_4(LS_3)L']^{2-}$ ($LS_3$ = 1,3,5-tris(4,6-dimethyl-3-mercaptophenylthio)-2,4,6-tris(*p*-tolylthio)benzene; L′ = Cl, SEt, SPh, 2-SPyr, Tp, $S_2CNEt_2$) clusters (Scheme 1).[11] These clusters were chosen based on the ability to replace the apical ligand (L′) preferentially, affording many derivatives for study. We also valued the ability of the $LS_3$ ligand to stabilize a [3Fe−4S] cluster after extrusion of the apical iron atom, a property we wished to explore in order to mimic the observed NO reactivity of mitochondrial aconitase.[7b] Altering L′ affects the denticity on the apical iron atom and further differentiates it from the remainder of the iron atoms in the cluster.

## EXPERIMENTAL SECTION

**General Procedures.** All manipulations were performed under an atmosphere of nitrogen gas using standard Schlenk techniques or in an MBraun glovebox under an atmosphere of purified nitrogen. NO (Airgas, 99%) was purified by a literature procedure.[12] The NO gas stream was passed through an Ascarite column (NaOH fused on silica gel) and a 6 ft coil filled with silica gel that was cooled to −78 °C using a dry ice/acetone bath. NO was stored using standard gas storage bulbs and transferred via gastight syringes. Diethyl ether, pentane, methylene chloride, and acetonitrile were purified using a Glass Contour solvent system. Deuterated solvents were purchased from Cambridge Isotope Laboratories Inc. (Tewksbury, MA). Compounds


dx.doi.org/10.1021/ic500586g | Inorg. Chem. 2014, 53, 5311−5320

**1**, **2a**, **2b**, **2d**, and **2e** (Scheme 1) and $Ph_3CSNO$ were synthesized according to literature procedures.[6a,11,13] All organic chemicals were purchased from Sigma-Aldrich and used as received. Metal salts were purchased from Strem Chemicals and used as received.

**Physical Measurements.** NMR spectra were recorded on a Bruker Avance spectrometer operating at 600 MHz at ambient temperature and referenced to residual signals in the deuterated solvent. Low-resolution electrospray ionization mass spectrometry (ESI-MS) spectra were obtained with an Agilent 1100 series LC/MSD mass spectrometer using degassed acetonitrile as the carrier solvent. FTIR spectra were recorded on a Thermo Nicolet Avatar 360 spectrometer running the *OMNIC* software package; solid samples were pressed into KBr disks, and solution samples were prepared in an airtight Graseby-Specac solution cell with $CaF_2$ windows and 0.1 mm spacers. In situ IR spectra were recorded on a ReactIR iC 10 instrument from Mettler Toledo equipped with a 1-in.-diameter, 30-reflection silicon ATR (SiComp) probe. In a typical experiment, the instrument was blanked with $CH_2Cl_2$ and the sample, at concentrations ranging from 15 to 30 mM. At the first data collection time point, NO(g) or a 30 mM $CH_2Cl_2$ solution of $Ph_3CSNO$ was added to the anaerobic sample compartment through a rubber septum via a gastight syringe. Samples for $^{57}$Fe Mössbauer studies were prepared by grinding a solid sample with Apiezon-N grease. These $^{57}$Fe Mössbauer samples were placed in an 80 K cryostat during measurement. A $^{57}$Co/Rh source was moved at a constant acceleration at room temperature against the absorber sample. All isomer shift ($\delta$) and quadrupole splitting ($\Delta E_Q$) values are reported with respect to $^{57}$Fe-enriched metallic iron foil that was used for velocity calibration. The displayed spectrum was folded to enhance the signal-to-noise ratio. Fits of the data were calculated by the *WMOSS* plot-and-fit program, version 2.5.[14] Samples for EPR data were prepared in 2-methyltetrahydrofuran. X-band EPR spectra were recorded on a Bruker EMX EPR spectrometer at ambient or liquid-nitrogen temperature using a quartz finger dewar. Electrochemical measurements were performed at ambient temperature in a glovebox on a VersaSTAT3 Princeton Applied Research potentiostat running the *V3-Studio* electrochemical analysis software. A three-electrode setup was employed comprising a glassy carbon working electrode, a platinum wire auxiliary electrode, and a Ag(s)/$Ag^+$(s) silver wire pseudoreference electrode. Triply recrystallized $(Bu_4N)PF_6$ was used as the supporting electrolyte. All electrochemical data were referenced internally to the $Fc/Fc^+$ couple at 0.00 V.

**X-ray Data Collection and Structure Solution and Refinement.** Crystals of **2c**·4MeCN·$Et_2O$·0.5$H_2O$, **2f**·2.5$Et_2O$, and $(Cp^*_2Fe)$**4** suitable for X-ray diffraction were mounted in Paratone N oil and frozen under a nitrogen cold stream maintained at 100 K by a KRYO-FLEX low-temperature apparatus. Data were collected on a Bruker APEX CCD X-ray diffractometer with Mo K$\alpha$ radiation ($\lambda$ = 0.71073 Å) controlled by the *APEX2* software package.[15] Empirical absorption corrections were calculated with *SADABS*.[16] The structures were solved by direct methods with refinement by full-matrix least squares based on $F^2$ using *SHELXTL-97*.[17] All non-hydrogen atoms were located and refined anisotropically. Hydrogen atoms were assigned to idealized positions and given thermal parameters equal to either 1.5 (methyl hydrogen atoms) or 1.2 (nonmethyl hydrogen atoms) times the thermal parameters of the atoms to which they were attached. Figures were generated using the Olex2 Graphical User Interface.[18] See Table 1 for crystallographic data and refinement details.

**Synthesis of $(Ph_4P)_2[Fe_4S_4(LS_3)N_3]$, 2c.** In a 25 mL Erlenmeyer flask, **1** (47.2 mg, 23.5 $\mu$mol) and $NaN_3$ (7.2 mg, 111 $\mu$mol) were combined. The mixture were dissolved in acetonitrile (14 mL) and then stirred at ambient temperature. After 18 h, the crude reaction solution was filtered through glass microfiber filter paper into a 125 mL Erlenmeyer flask. The filtrate was stripped to dryness and the resulting solid dissolved in acetonitrile (3 mL). The solution was layered with diethyl ether (45 mL) and placed in a −30 °C freezer overnight to afford a precipitate, which was collected on an F-grade frit and washed with diethyl ether (3 × 10 mL) to yield 29.3 mg (14.5 $\mu$mol, 58.2%) of blue-black microcrystalline material. Crystals suitable for X-ray diffraction studies were grown by vapor diffusion of diethyl ether into an acetonitrile solution of **2c**. The $^1$H NMR spectrum matched that previously published.[19] $^1$H NMR (600 MHz, $CD_3CN$, $\delta$ ppm): 8.25 (5-H), 7.13 (2′-H), 6.83 (3′-H), 5.05 (br, 2-H), 3.90 (4-Me), 3.87 (6-Me), 2.24 (4′-Me). Anal. Calcd for $C_{95}H_{87}Fe_4N_3P_2S_{13}O$: C, 58.37; H, 4.31; N, 2.06. Found: C, 58.34; H, 4.47; N, 1.82. ESI-MS (MeCN, $m/z$): 339.2 ($[Ph_4P]^+$, calcd 339.1), 1678.7 ($[M - Ph_4P]^-$, calcd 1678.9), 669.6 ($[M - 2(Ph_4P)]^{2-}$, calcd 669.4). FTIR (KBr, $cm^{-1}$): 2906 (w), 2055 (s, $\nu_{azide}$), 1585 (w), 1488 (w), 1435 (s), 1377 (w), 1336 (w), 1258 (w), 1185 (w), 1107 (s), 1079 (s), 1028 (w), 996 (w), 954 (w), 872 (w), 801 (w), 751 (w), 722 (s), 688 (s), 526 (s).

**Synthesis of $(Ph_4P)_2[Fe_4S_4(LS_3)(S_2CNEt_2)]$, 2f.** In a 25 mL Erlenmeyer flask, **1** (104.6 mg, 52 $\mu$mol) and $NaS_2CNEt_2$ (10.0 mg, 58.4 $\mu$mol) were combined. The solid mixture was dissolved in acetonitrile (8 mL) and stirred. After 4 h, the crude reaction solution was filtered through glass microfiber filter paper into a 125 mL Erlenmeyer flask. The filtrate was stripped to dryness and redissolved in acetonitrile (3 mL). The solution was layered with diethyl ether (120 mL) and placed in a −30 °C freezer overnight to afford a precipitate, which was collected on an F-grade frit and washed with diethyl ether (3 × 10 mL) to yield 83.8 mg (38.9 $\mu$mol, 74.8%) of black microcrystalline material. Crystals suitable for X-ray diffraction studies were grown by vapor diffusion of diethyl ether into a *N*,*N*-dimethylformamide solution of **2f**. The $^1$H NMR spectrum matched the published one.[11c] $^1$H NMR (600 MHz, $CD_3CN$, $\delta$ ppm): 8.26 (5-H), 7.20 (2′-H), 7.01 ($CH_2$), 6.74 (3′-H), 4.89 (br, 2-H), 3.88 (6-Me), 3.64 (4-Me), 2.27 (4′-Me), 1.27 ($CH_3$). Anal. Calcd for $C_{104}H_{95}Fe_4NP_2S_{15}$·2$Et_2O$: C, 59.17; H, 5.10; N, 0.62. Found: C, 59.42; H, 5.15; N, 0.53. ESI-MS (MeCN, $m/z$): 339.4 ($[Ph_4P]^+$, calcd 339.1), 1446.0 ($[M - 2(Ph_4P)]^-$, calcd 1445.8). FTIR (KBr, $cm^{-1}$): 2908 (w), 1585 (w), 1524 (w), 1483 (s), 1435 (s), 1375 (w), 1354 (w), 1266 (w), 1210 (w), 1139 (w), 1107 (s), 1078 (s), 1014 (w), 996 (w), 955 (w), 800 (w), 752 (w), 722 (s), 688 (s), 506 (s). $^{57}$Fe Mössbauer (80 K, $\delta$ mm/s, $\Delta E_Q$ mm/s, $\Gamma$ mm/s, area %): (site 1) 0.71(2), 2.06(2), 0.31(2), 20; (site 2) 0.46(2), 1.12(2), 0.34(2), 80.

**NO(g) Reactions.** In a 20 mL vial, **1** or **2a**−**2f** (20.8 $\mu$mol) was dissolved in methylene chloride (6 mL), and the vial was sealed with a rubber septum. A total of 1 equiv of NO(g) (500 $\mu$L, 16.35 $\mu$mol) was then injected via a gastight syringe into the reaction vial. The reaction was stirred for 2 h and subsequently poured into pentane (120 mL) and stirred for 10 min. The mixture was filtered over Celite, and the residual solid was extracted with methylene chloride (50 mL). After solvent removal, the remaining solid was characterized by ESI-MS and $CH_2Cl_2$ solution FTIR. Formation of $[Fe_4S_4(NO)_4]^-$, **4**, and $[Fe_4S_3(NO)_7]^-$, RBA, was observed.

**$Ph_3CSNO$ Reactions.** In a 20 mL vial, **1** or **2a**−**2f** (16.35 $\mu$mol) were dissolved in methylene chloride (6 mL), and the vial was sealed with a rubber septum. In a 5 mL vial, 1, 2, 4, or 8 equiv of $Ph_3CSNO$ (16.35, 32.7, 65.4, and 130.8 $\mu$mol, respectively) was dissolved in methylene chloride (5 mL) and instantly injected via syringe into the reaction vial. Throughout the course of the reaction, 40−60 $\mu$L aliquots were taken to monitor the reaction by solution IR. After no further growth of the bands in the region between 1600 and 1850 $cm^{-1}$ was observed (2−6 h), the reaction mixture was poured into pentane (120 mL) and stirred for 10 min. The mixture was filtered over Celite. The filtrate was analyzed by gas chromatography−mass spectrometry (GC−MS) to reveal the formation of $(Ph_3CS)_2$ and by $^1$H NMR spectroscopy in $CD_3CN$ to show the presence of the $LS_3$ ligand. The solid remaining on the Celite was extracted with methylene chloride (50 mL). After solvent removal, the remaining solid was characterized by ESI-MS, Mössbauer, $CH_2Cl_2$ solution FTIR, and KBr solid-state FTIR. If up to 4 equiv of $Ph_3CSNO$ were used, the isolated nitrosated product was **4**. When 8 equiv of $Ph_3CSNO$ were used, the isolated product was RBA.

**Synthesis of $[(C_5Me_5)_2Fe][Fe_4S_4(NO)_4]$, $(Cp^*_2Fe)$[4].** In a 20 mL vial, **1** (32.9 mg, 16.4 $\mu$mol) and $TlPF_6$ (28.4 mg, 81.3 $\mu$mol) were dissolved in methylene chloride (6 mL). The reaction vial was sealed with a septum. In a 5 mL vial, $Ph_3CSNO$ (20.0 mg, 65.4 $\mu$mol) was dissolved in methylene chloride (5 mL) and instantly injected via syringe into the reaction vial. After 2 h, the reaction mixture was


dx.doi.org/10.1021/ic500586g | *Inorg. Chem.* 2014, 53, 5311−5320

poured into pentane (120 mL) and stirred for 10 min. The mixture was filtered over Celite, and the filtrate was stripped to yield 30.4 mg of a yellow-brown solid. Characterization of the mixture using ESI-MS, $CH_2Cl_2$ solution FTIR, and cyclic voltammetry confirmed the presence of $[Fe_4S_4(NO)_4]$, **3**. This solid mixture was dissolved in methylene chloride (2 mL), and $(C_5Me_5)_2Fe$ (22.3 mg) was added. The reaction was stirred for 30 min and subsequently poured into pentane (100 mL), affording a black precipitate. The precipitate was collected via filtration over Celite and extracted with methylene chloride (10 mL). The methylene chloride solution was stripped to yield 8.3 mg (10.0 $\mu$mol, 61.0%) of a black powder. Crystals suitable for X-ray diffraction studies were grown by vapor diffusion of diethyl ether into a methylene chloride solution of $(Cp^*_2Fe)$**4**. ESI-MS (MeCN, $m/z$): 326.2 ($(Cp^*_2Fe)^+$, 326.3), 471.6 ($[\mathbf{4}]^-$, 471.6), 441.5 ($[\mathbf{4-NO}]^-$, 441.6), 411.5 ($[\mathbf{4-2NO}]^-$, 411.6), 381.5 ($[\mathbf{4-3NO}]^-$, 381.6), 351.5 ($[\mathbf{4-4NO}]^-$, 351.6). FTIR ($CH_2Cl_2$, $cm^{-1}$): 1725 (s, $\nu_{NO}$). Anal. Calcd for $C_{20}H_{30}Fe_5S_4N_4O_4$: C, 30.10; H, 3.79; N, 7.02. Found: C, 30.04; H, 3.41; N, 6.80.

## RESULTS AND DISCUSSION

**Synthesis and Characterization of Clusters.** Over the course of two decades, numerous ligand substitutions were carried out on the site-differentiated, apical iron atom of $[Fe_4S_4(LS_3)L']^{2-}$.[20] All transformations here began with **1** and were performed using alkali metal salts of the ligands in organic solvents. The use of alkali metals to precipitate MCl (where M is $Na^+$ or $K^+$) drives the reaction toward completion by replacing the ligand on the apical iron atom to afford the ligand-substituted product as microcrystalline material in 50−90% yield and an insoluble alkali halide salt.

Characterization of these clusters by $^1$H NMR spectroscopy is possible owing to the $S = 0$ ground state of their $[Fe_4S_4]^{2+}$ cores. The chemical shifts of the protons appear downfield from those of the free ligand, and their line widths are broadened from what would be expected of a diamagnetic complex, suggesting that thermal excitation produces a weakly paramagnetic state. Electronic effects imparted by varying the apical ligand are manifest in different chemical shifts, especially of protons closest in proximity to the cluster. As a result, distinct $^1$H NMR spectra can be obtained for almost every compound. These complexes were also identified by ESI-MS, with mass peaks corresponding to $[M-Ph_4P]^-$ being common and additional peaks arising from the presence of $[M - 2Ph_4P]^{2-}$. IR spectroscopy is useful in identifying the formation of **2c** by the $\nu_{azide}$ stretch at 2055 $cm^{-1}$ but does not provide information about the extent of substitution. Shifts in the IR bands of the derivatives of **1** are minimal and not useful in assessing conversion.

The synthesis of **2c** has been previously reported using $Me_3SiN_3$ as the azide source.[19] We report the formation of **2c** using excess $NaN_3$ over the course of 18 h. This synthesis is more convenient than the previously published route. Sodium azide is readily available and is not as dangerous as the silane. The $^1$H NMR spectrum of **2c** is identical to that in starting complex **1**, preventing us from monitoring the reaction completion by this technique, as was the case for other $[Fe_4S_4(LS_3)L']^{2-}$ products. Conversion of the apical ligand from $Cl^-$ to $N_3^-$ can, however, be followed using ESI-MS, observing the decrease of a peak at $m/z$ 1672.6 and formation of one at $m/z$ 1678.7.

The X-ray crystal structure of **2c** (Figure 2) reveals an almost linear azide ion [N−N−N = 177.2(9)°] with a bent coordination geometry at the apical iron atom [Fe−N−N = 132.4(6)°]. The three *p*-tolyl groups of the $LS_3$ ligand are oriented away from the cluster, a result that differs from the published structure of **1** but which most likely arises owing to packing of cocrystallized molecules of acetonitrile occupying the voids created by these aryl groups in the crystal lattice.[11b] A water molecule in the lattice was introduced during the refinement to account for residual electron density in the lattice. It was refined with disorder about a special position and may have arisen from residual water in the acetonitrile solvent.

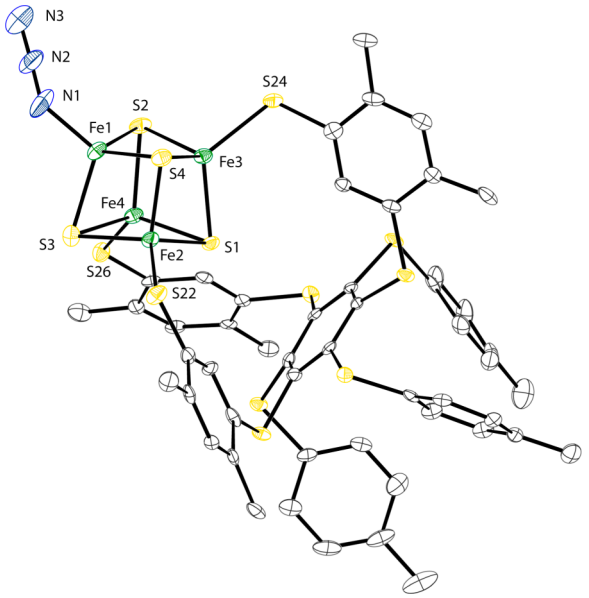


**Figure 2.** Drawing of the X-ray crystal structure of $[Fe_4S_4(LS_3)(N_3)]^{2-}$, **2c**, with ellipsoids shown at 50% occupancy. Cations, solvent molecules, and hydrogen atoms are omitted for clarity. Color coding: iron, green; sulfur, yellow; nitrogen, blue; carbon, colorless.

The formation of **2f** was previously observed by $^1$H NMR spectroscopy and cyclic voltammetry, but it was never isolated and characterized. The synthesis of the $(Ph_4P)_2[Fe_4S_4(LS_3)(S_2CNMe_2)]$ analogue was published, but an X-ray crystal structure was never obtained, resulting in some ambiguity as to whether the apical iron atom is four- or five-coordinate. We have isolated **2f** in high yield and were able to obtain X-ray-diffraction-quality crystals (Figure 3).

The apical iron is five-coordinate with asymmetric thiocarbamate sulfur atoms, S71 and S72, at distances from the apical iron of 2.3918(10) and 2.6063(10) Å, respectively. As in **2c**, the *p*-tolyl groups of the $LS_3$ ligand in **2f** are oriented away from the cluster, but with the aryl rings of the $(Ph_4P)^+$ cation partially occupying the voids. The refined structure has high residual electron density (2.322 e/Å$^3$) near an oxygen atom of one of the $Et_2O$ molecules at a site of positional disorder that could not be refined satisfactorily.

The Mössbauer spectrum of **2f** (Figure 4) shows that the apical iron atom is electronically differentiated from the remainder of the cluster. This differentiation is typically observed when the apical ligand is multidentate (as in the case of **2d** and **2e**).[11a]

**Reactions with NO(g).** In the substoichiometric reaction of clusters **1** and **2a**−**2f** with 1 equiv of NO(g), two nitrosyliron species (eq 1) are observed by IR spectroscopy and ESI-MS (Figure 5) along with the starting cluster. The first species is RBA, as evidenced by $\nu_{NO}$ bands at 1797, 1742, and 1705 $cm^{-1}$ ($CH_2Cl_2$) and observed masses for $[Fe_4S_3(NO)_x]^-$, where $x$


dx.doi.org/10.1021/ic500586g | Inorg. Chem. 2014, 53, 5311−5320

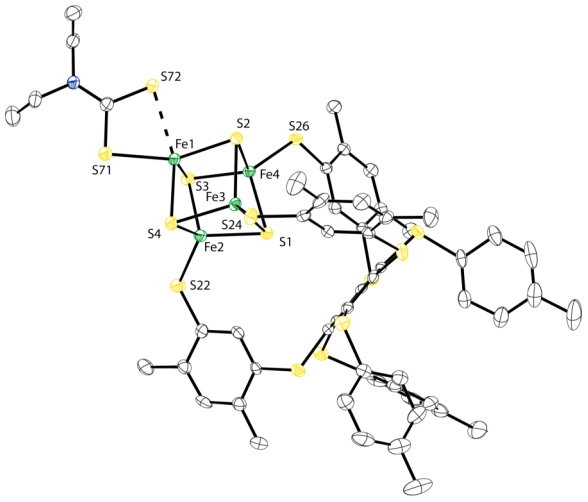


**Figure 3.** Drawing of the X-ray crystal structure of $[Fe_4S_4(LS_3)(S_2CNEt_2)]^{2-}$, **2f**, with ellipsoids shown at 50% occupancy. Cations, solvent molecules, and hydrogen atoms are omitted for clarity. Color coding: iron, green; sulfur, yellow; nitrogen, blue; carbon, colorless.

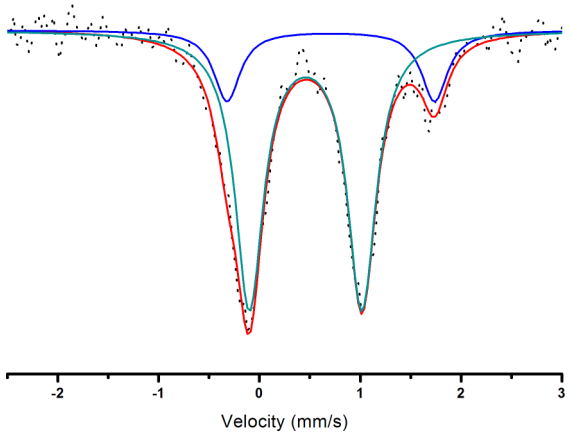


**Figure 4.** Mössbauer spectrum of **2f** collected at 80 K with a two-site fit (black dots, raw data; red line, two-site fit; green line, site 1 fit; blue line, site 2 fit).

ranges from 1 to 7.[21] The formation of RBA was anticipated because it has been identified as the dominant nitrosyliron product in the reaction of NO(g) and $Ph_3CSNO$ with $[Fe_4S_4(SPh)_4]^{2-}$ and other synthetic iron–sulfur clusters.[6a] The second nitrosyliron species was identified as **4**, based on a $\nu_{NO}$ band at 1725 $cm^{-1}$ ($CH_2Cl_2$) and observed masses for $[Fe_4S_4(NO)_y]^-$, where $y$ ranges from 0 to 4 (Figure 5).[22] In situ monitoring of the reaction by ReactIR showed concomitant formation of both species (Figure S16 in the Supporting Information, SI). Upon addition of 8 equiv of NO(g), the sole nitrosyliron product is RBA.

$$2[Fe_4S_4(LS_3)Cl]^{2-} + 11NO(g) \rightarrow [Fe_4S_4(NO)_4]^- + [Fe_4S_3(NO)_7]^- + 2Cl^- + S^0 + (LS_3)_2 \quad (1)$$

This result differs from that in previously published work, which reported the formation of only RBA from synthetic, undifferentiated [4Fe–4S] clusters even in the presence of only 1 equiv of NO(g).[6a] Our results suggest that the tridentate character of the $LS_3$ ligand may slow the reaction kinetics of these clusters with NO(g) by inhibiting its access to the less exposed iron sites of the cluster.

**Reactions with $Ph_3CSNO$.** In an attempt to control the release of NO and isolate possible intermediate species, the *S*-nitrosothiol $Ph_3CSNO$ was allowed to react with clusters **1** and **2a–2f**. When monitoring the cluster reaction with 1–4 equiv of $Ph_3CSNO$ by solution FTIR and ReactIR spectroscopy, the sole nitrosyliron product observed was **4** (eq 2), which is in contrast to the reaction of $(Et_4N)_2[Fe_4S_4(SPh)_4]$ with 1 equiv of $Ph_3CSNO$, forming RBA (Figure 6). After addition of 2 equiv of $Ph_3CSNO$, the unreacted cluster was still observed by ESI-MS and Mössbauer spectroscopy. Upon addition of 4 equiv of $Ph_3CSNO$, only **4** was observed in the mass and Mössbauer spectra (Figure 7). Further addition to a combined total of 8 equiv of $Ph_3CSNO$ results in the conversion of **4** into RBA (eq 3). This conversion was previously observed while trying to obtain X-ray-quality crystals of $[AsPh_4]$**4**, but only $[AsPh_4]$RBA was isolated, formed presumably by an unknown decomposition pathway. Formation of **4** has not been reported to occur during nitrosation of $[Fe_4S_4(SR)_4]^{2-}$ clusters.[23] Formation of RBA from **4** has also been observed upon one-electron oxidation of **4** to **3** followed by air exposure.[24] This known reaction pathway suggests that **4** may form in biology at low NO concentrations from [4Fe–4S] clusters but then

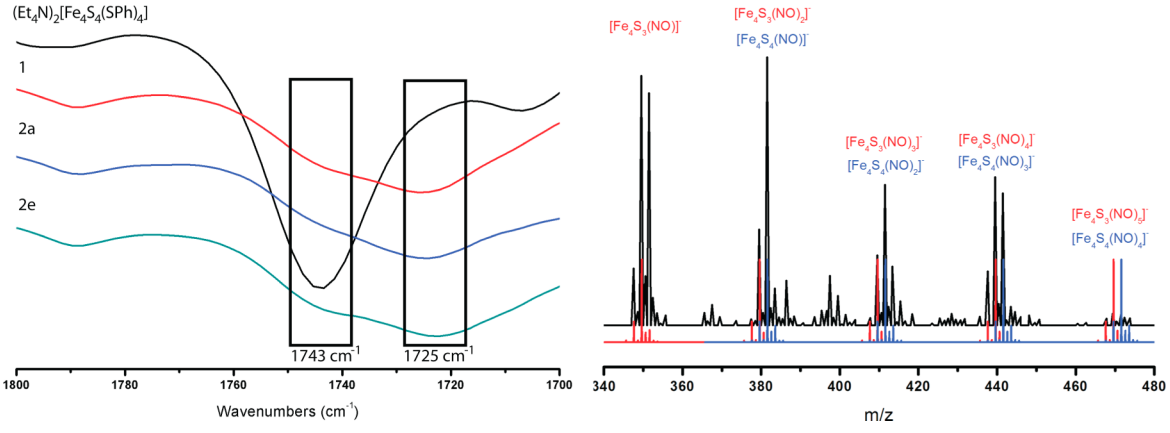


**Figure 5.** Characterization of the products formed between clusters and NO(g). Left: $CH_2Cl_2$ solution IR spectra. Right: ESI-MS negative-mode spectrum from the reaction of **2b** (black, experimental; red, simulated $[Fe_4S_3(NO)_x]^-$; blue, simulated $[Fe_4S_4(NO)_x]^-$).


dx.doi.org/10.1021/ic500586g | Inorg. Chem. 2014, 53, 5311–5320

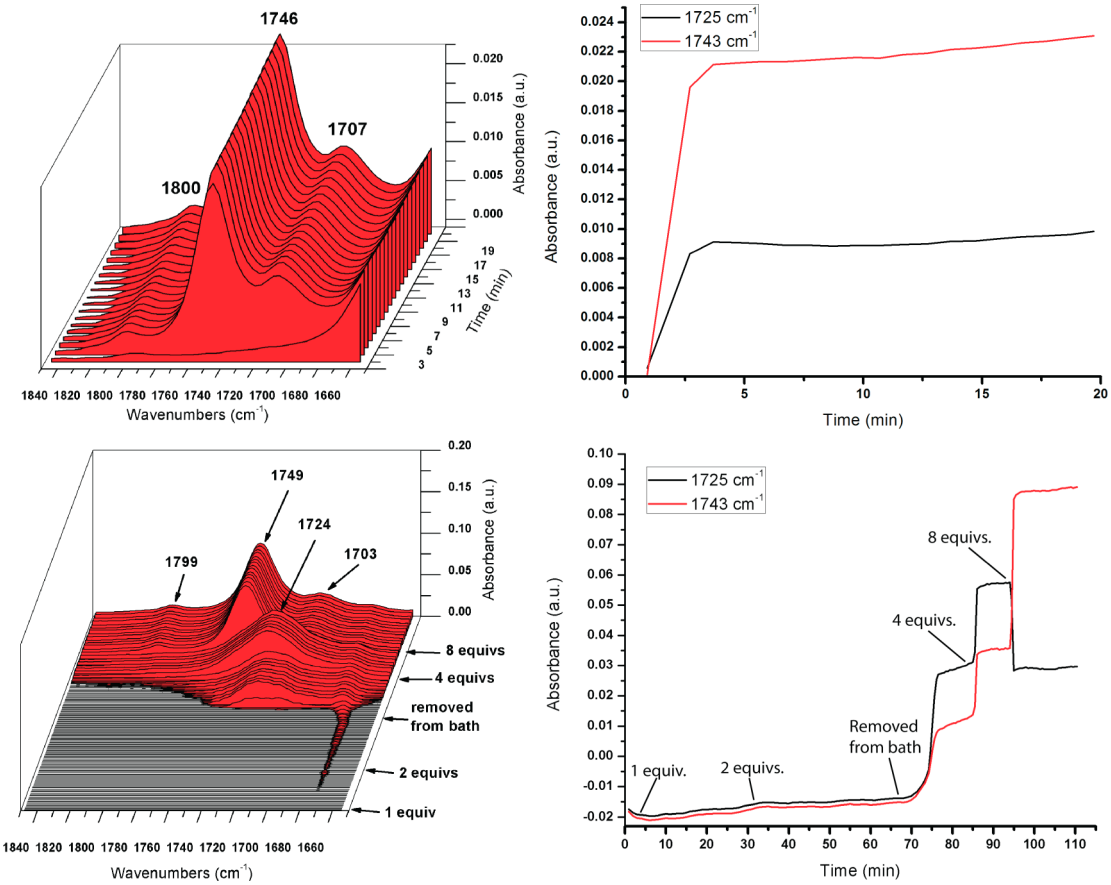


**Figure 6.** ReactIR spectra of $(Et_4N)_2[Fe_4S_4(SPh)_4]$ and 1 equiv of $Ph_3CSNO$ in $CH_2Cl_2$ at ambient temperature (top), **2b**, and varying equivalents of $Ph_3CSNO$ (bottom). The time-dependent absorbances at different wavenumbers were monitored to observe the formation of **4** en route to RBA, which did not occur in the $[Fe_4S_4(SPh)_4]^{2-}$ reaction (top) but did in the reaction of **2b** (bottom). The **2b** solution was initially maintained in a dry ice/acetone bath, but after no detectable product formed after 1 h, the reaction was removed from the bath and allowed to warm to room temperature.

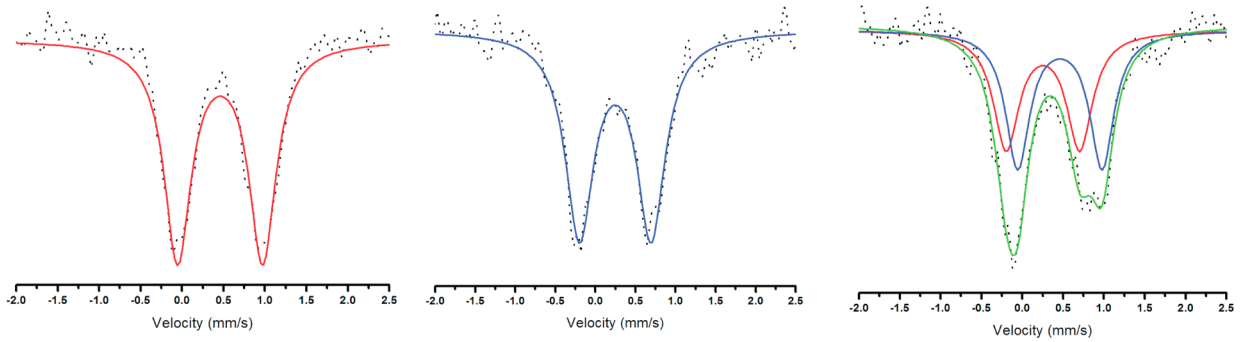


**Figure 7.** 80 K Mössbauer spectrum of **1** (left; raw data, black dots; fitted spectrum, red line), **4** (middle; raw data, black dots; fitted spectrum, blue line), and **1** and **4** via the reaction with 2 equiv of $Ph_3CSNO$ (right; raw data, black dots; fitted spectrum, green line; **1**, red line; **4**, blue line). Mössbauer parameters for each spectrum are given in Table 2

convert readily to RBA in the presence of cellular oxidants and oxygen.

$$[Fe_4S_4(LS_3)Cl]^{2-} + 4Ph_3CSNO \rightarrow [Fe_4S_4(NO)_4]^{-} + Cl^{-} + \frac{1}{2}(LS_3)_2 + 2(Ph_3CS)_2 \quad (2)$$

$$[Fe_4S_4(LS_3)Cl]^{2-} + 7Ph_3CSNO \rightarrow [Fe_4S_3(NO)_7]^{-} + Cl^{-} + S^0 + \frac{1}{2}(LS_3)_2 + 3.5(Ph_3CS)_2 \quad (3)$$

The reactions were worked up by pouring the mixture into a 10-fold excess volume of pentanes, filtering over Celite, and extracting the remaining solid with methylene chloride. Solvent was removed from the filtrate and the methylene chloride extract to afford products weighing 26.4 and 17.2 mg,


dx.doi.org/10.1021/ic500586g | Inorg. Chem. 2014, 53, 5311−5320

**Table 2. Mössbauer Parameters of Relevant Iron−Sulfur Complexes**

| complex | temperature (K) | isomer shift ($\delta$, mm/s) | quadrupole splitting ($\Delta_{EQ}$, mm/s) | line width ($\Gamma$, mm/s) | area (%) | ref |
|---|---|---|---|---|---|---|
| **4** | 80 | 0.25(2) | 0.90(2) | 0.42(2) | 100 | this work |
| **1** + **4** | 80 | 0.25(2) | 0.90(2) | 0.38(2) | 48 | this work |
| | | 0.46(2) | 1.03(2) | 0.36(2) | 52 | |
| [K(2,2,2-crypt)]**4** | 300 | 0.156 | 0.935 | N/A | 100 | 22 |
| $[Fe_4S_4(NO)_4]$, **3** | 78 | 0.150 | 1.473 | 0.334 | 100 | 26 |
| $(Et_4N)[Fe_4S_3(NO)_7]$, RBA | 90 | 0.15(2) | 0.97(2) | 0.32(2) | 100 | 9a |
| $(Et_4N)[Fe(SPh)_2(NO)_2]$ | 90 | 0.17(2) | 0.68(2) | 0.26(2) | 100 | 9a |
| $Fe(NO)(S_2CNEt_2)_2$ | 300 | 0.51(1) | 0.80(1) | N/A | 100 | 27 |
| $(Ph_4P)_2[Fe_4S_4(LS_3)Cl]$, **1** | 80 | 0.46(2) | 1.03(2) | 0.39(2) | 100 | this work |
| $(Ph_4P)_2[Fe_4S_4(LS_3)(SEt)]$, **2a** | 80 | 0.44(2) | 0.90(2) | 0.36(2) | 60 | this work |
| | | 0.44(2) | 1.21(2) | 0.27(2) | 40 | |
| $(Ph_4P)_2[Fe_4S_4(LS_3)(S_2CNEt_2)]$, **2f** | 80 | 0.71(2) | 2.06(2) | 0.31(2) | 20 | this work |
| | | 0.46(2) | 1.12(2) | 0.34(2) | 80 | |

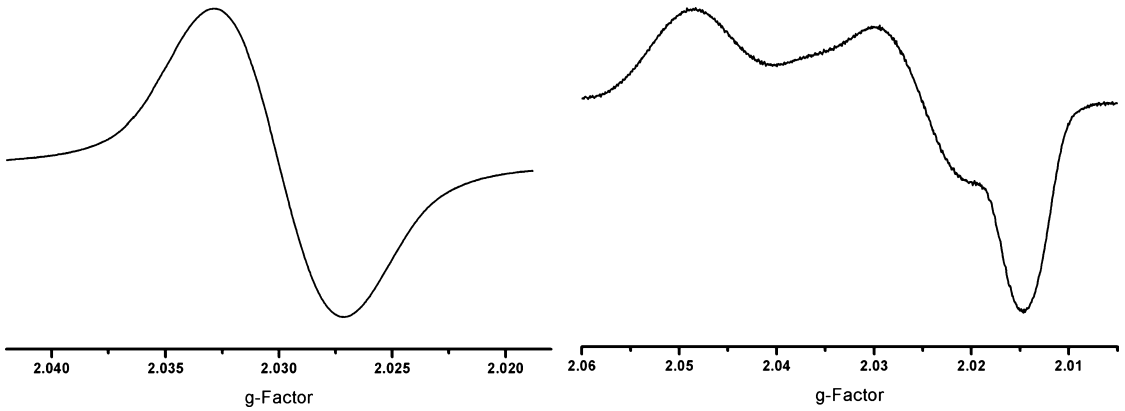


**Figure 8.** X-band EPR spectra of **4** at room temperature (left) and 77 K (right). Conditions: RT, frequency 9.847 GHz, microwave power 2.017 mW, modulation amplitude 10.0 G; 77 K, frequency 9.208 GHz, microwave power 1.992 mW, modulation amplitude 10.0 G. The RT spectrum is an isotropic $S = {}^1/_2$ signal with $g_{avg} = 2.030$. The 77 K spectrum is a rhombic $S = {}^1/_2$ signal with $g_1 = 2.014$, $g_2 = 2.026$, and $g_3 = 2.049$. The shape and $g$ values of both spectra are typically associated with DNICs in the literature.

respectively. These masses may correspond to the $LS_3$ ligand and $(Ph_3CS)_2$ in the filtrate and $(Ph_4P)Cl$ and **4** in the methylene chloride. The expected masses are 33.5 mg for the filtrate and 19.4 mg for the methylene chloride extract. The presence of the $LS_3$ ligand and $(Ph_3CS)_2$ in the filtrate was confirmed by $^1H$ NMR spectroscopy. The formation of $(Ph_3CS)_2$ was further evidenced by GC−MS and X-ray crystallography (Figures S29 and S43 in the SI). Separation of **4** and $(Ph_4P)Cl$ obtained from the methylene chloride extract was not achieved, but spectroscopic characterization of **4** was not affected by this impurity.

The 80 K Mössbauer spectrum of the methylene chloride extract shows a doublet with an isomer shift of 0.25 mm/s (Figure 7). This value differs from the published one for [K(2,2,2-crypt)]**4** at 300 K (0.156 mm/s) but is close to the temperature-corrected value at 4.2 K (0.27 mm/s).[22,25] The observed quadruple splitting of **4** at 80 K is 0.90 mm/s, in agreement with the previously reported value of 0.935 mm/s at 300 K of [K(2,2,2-crypt)]**4**. The slight variations in isomer shifts may be due to temperature differences, but they are nonetheless distinct from values of other known iron nitrosyl species and the starting materials used in this work (Table 2).[26] The Mössbauer spectrum of **4** also appears, in a 1:1 ratio with the starting material, in a methylene chloride extract of the reaction of **1** with 2 equiv of $Ph_3CSNO$, providing further evidence that at substoichiometric amounts of $Ph_3CSNO$ the only observable product is **4**.

An X-band EPR spectrum of the sample recorded at ambient temperature exhibited an isotropic signal with $g_{avg} = 2.030$, and at 77 K a rhombic signal appeared with $g_1 = 2.014$, $g_2 = 2.026$, and $g_3 = 2.049$ (Figure 8). These spectra have features similar to those in published EPR spectra of biological DNICs, suggesting that previously reported experiments describing the formation of DNICs were potentially observations of **4**.[7a,28] This conclusion may apply particularly when products of [4Fe−4S] cluster nitrosation were assigned by their EPR spectra as non-protein-bound DNICs. In a previous NRVS study using recombinant *Pyrococcus furiosus* ferredoxin (D14C mutant), RBA was identified as the major nitrosated product upon exposure to propylammonium NONOate.[9a] A minor EPR-active byproduct having $g_{avg} = 2.03$ was assigned as a protein-bound DNIC. Our current findings suggest that this and other results merit reconsideration. Further investigation of low-molecular-weight products of protein nitrosations using MS, IR, NRVS, and Mössbauer spectroscopy are required to improve our understanding of the nitrosated products.[29]

Diamagnetic nitrosated products have been identified in stopped-flow kinetic studies of two proteins of the Wbl family.[5a,b] This study reported evidence that the final product was generated via the formation of mono-, di-, and tetranitrosated intermediates. The absence of additional


dx.doi.org/10.1021/ic500586g | Inorg. Chem. 2014, 53, 5311−5320

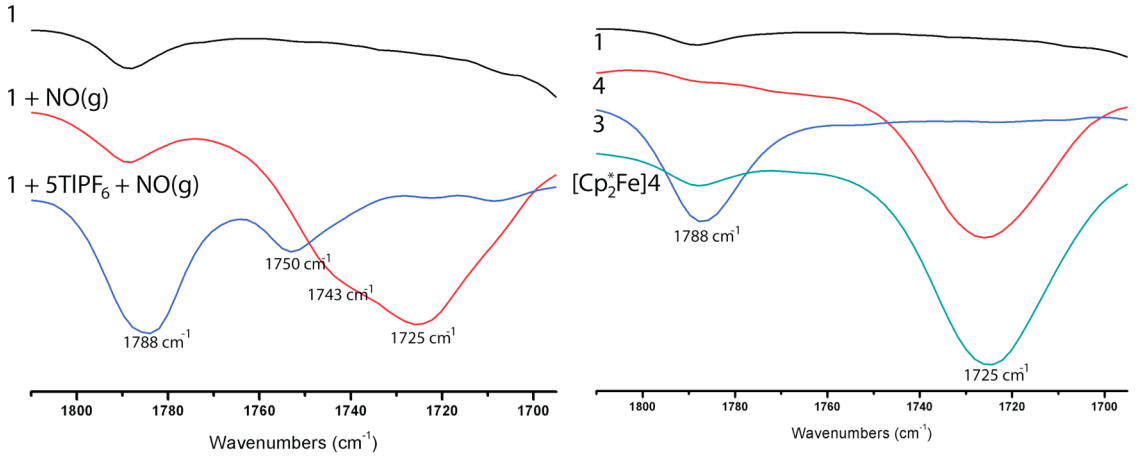


**Figure 9.** $CH_2Cl_2$ solution FTIR of the reaction of **1** in the presence of excess $TlPF_6$ and 1 equiv of NO(g) (left) and $Ph_3CSNO$ (right).

vibrational bands in the ReactIR traces during the present investigation, even at low temperature, suggests that isolation and characterization of a mono- or dinitrosated iron−sulfur cubane cluster will be a difficult task. The instability of these thiol-bound, partially nitrosated cubane clusters may lead to complete extrusion of the cluster from the $LS_3$ ligand, as previously reported using $^t$BuS$^-$.[11b]

**Reactions with NO(g)/$Ph_3CSNO$ in the Presence of $TlPF_6$.** Efforts to isolate a mononitrosated cubane were unsuccessful. When attempts were made to identify a $[Fe_4S_4(LS_3)(NO)]^{x-}$ species from the reaction of **1** and $Ph_3CSNO$ in the presence of a 5-fold excess of $TlPF_6$, a $\nu_{NO}$ band at 1790 cm$^{-1}$ ($CH_2Cl_2$) was observed in the IR spectrum. This species was subsequently identified as $Fe_4S_4(NO)_4$, **3**, by cyclic voltammetry and ESI-MS (SI). Cyclic voltammetry shows two reversible reductions centered at −314 and −1097 mV, which match the literature values of −370 and −1150 mV for this compound.[22] The reaction of **1** and NO(g) in the presence of $TlPF_6$ yields **3** and RBA (eq 4 and Figure 9). Compound **3** can also be obtained by addition of a 5-fold excess of $TlPF_6$ after formation of **4** from **1** (eq 5) or **2a**/**2b**.

$$2[Fe_4S_4(LS_3)Cl]^{2-} + 11NO(g) + 3Tl^+ \rightarrow [Fe_4S_4(NO)_4] + [Fe_4S_3(NO)_7]^- + 2TlCl(s) + (LS_3)_2 + S^0 + Tl(s) \quad (4)$$

$$[Fe_4S_4(LS_3)Cl]^{2-} + 4Ph_3CSNO + 2Tl^+ \rightarrow [Fe_4S_4(NO)_4] + TlCl(s) + \frac{1}{2}(LS_3)_2 + 2(Ph_3CS)_2 + Tl(s) \quad (5)$$

The one-electron reduction of **3** using $(C_5Me_5)_2Fe$ resulted in formation of $(Cp^*_2Fe)$[**4**] (Figure 10). This complex was crystallized from $CH_2Cl_2/Et_2O$ with two independent molecules in the asymmetric unit. The bond lengths and angles of the cluster are comparable to those published for [K(2,2,2-crypt)][**4**] and other mononitrosyl-capped iron−sulfur clusters (Table 3). The observed isotopic patterns in the MS spectrum and the $\nu_{NO}$ band in the IR match published values and those observed in direct reactions of **1** with $Ph_3CSNO$, providing further proof that the major isolatable product of stoichiometric nitrosation of $[Fe_4S_4(LS_3)L']^{2-}$ is **4**.

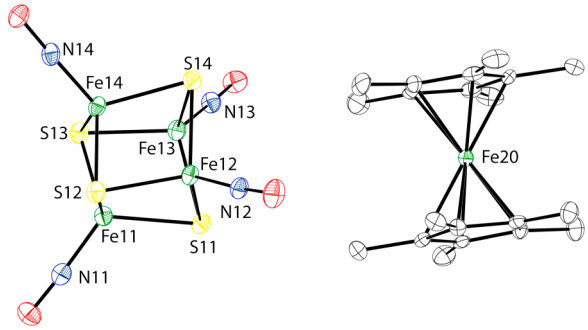


**Figure 10.** Drawing of $(Cp^*_2Fe)$[**4**] with 50% probability thermal ellipsoids. The other complex in the asymmetric unit and hydrogen atoms are omitted for clarity. Color coding: iron, green; sulfur, yellow; nitrogen, blue; oxygen, red; carbon, colorless.

## CONCLUSIONS

The reactions of the site-differentiated clusters **1** and **2a**−**2f** with either NO(g) or $Ph_3CSNO$ produce the $S = {}^1/_2$ nitrosated cluster **4** en route to the formation of the diamagnetic RBA. The transformation of **4** into RBA by addition of an oxidant has been observed previously,[23] but the present study is the first to demonstrate that nitrosation of [4Fe−4S] clusters proceeds through **4** en route to the RBA. The tetranitrosated cluster has an EPR spectrum similar to that typically associated with DNICs but exhibits only a single $\nu_{NO}$ band in the IR spectrum as well as different Mössbauer parameters. The detection and isolation of EPR-active **4** via the direct reaction of [4Fe−4S] clusters with NO suggest that some nitrosyliron products previously reported in the literature may have been mischaracterized as DNICs. This result is of particular interest when most of the nitrosated products are EPR-silent, suggesting formation of RBA as the end product. Further investigations of low-molecular-weight nitrosyliron products by methods other than EPR are necessary to determine conclusively whether **4** or a DNIC is generated in a biological setting.

The isolation of a partially nitrosated cluster was not achieved. Even in the presence of thallium added to remove the apical chloride ion, the cluster was oxidized by $Tl^+$ to form **3**, which was then used to form $(Cp^*_2Fe)$[**4**] for crystallographic verification of the formation of **4**.


dx.doi.org/10.1021/ic500586g | Inorg. Chem. 2014, 53, 5311−5320

Table 3. Geometric Parameters of Iron−Sulfur Clusters Capped with mononitrosyls

| | $(Cp_2^*Fe)[4]$ | $[K(2,2,2\text{-crypt})][4]$[22] | 3[22] | $(Me_4N)_2[Fe_4S_4(NO)_4]$[6b] | $(PPN)_2[Fe_8S_6(NO)_8]$[30] |
|---|---|---|---|---|---|
| | | | Bond Length, Å | | |
| Fe−N | 1.654(4); 1.655(4) | 1.655(5) | 1.661(5) | 1.665(6) | 1.673(3) |
| | 1.658(4); 1.664(4) | 1.659(5) | 1.662(6) | 1.665(7) | 1.674(2) |
| | 1.660(4); 1.664(4) | 1.660(5) | 1.663(5) | | 1.676(2) |
| | 1.665(4); 1.665(4) | 1.663(5) | 1.666(6) | | 1.676(2) |
| N−O | 1.176(4); 1.175(4) | 1.162(6) | 1.143(6) | 1.181(9) | 1.177(2) |
| | 1.183(4); 1.179(4) | 1.166(6) | 1.148(7) | 1.193(9) | 1.179(3) |
| | 1.185(4); 1.180(4) | 1.167(6) | 1.157(6) | | 1.179(4) |
| | 1.192(4); 1.189(4) | 1.178(6) | 1.171(6) | | 1.184(3) |
| | | | Bond Angle, deg | | |
| Fe−N−O | 175.8(3); 175.8(3) | 176.8(5) | 176.9(5) | 176.4(6) | 174.6(2) |
| | 176.7(3); 176.8(3) | 176.9(5) | 177.3(5) | 176.7(6) | 176.7(2) |
| | 178.1(4); 177.9(3) | 177.4(4) | 177.6(5) | | 178.1(2) |
| | 179.1(3); 179.1(3) | 178.9(6) | 178.8(5) | | 178.8(2) |

## ■ ASSOCIATED CONTENT

### Supporting Information

IR and ESI-MS spectra of all NO(g) and $Ph_3CSNO$ reactions, $^1H$ NMR spectra of clusters **1**, **2a**−**2f**, GC−MS of the pentane soluble product of **1** + $Ph_3CSNO$, cyclic voltammogram of **3**, full depictions of the asymmetric units of the crystal structures, and CIF files. This material is available free of charge via the Internet at http://pubs.acs.org.

## ■ AUTHOR INFORMATION


### Corresponding Author

*E-mail: lippard@mit.edu. Phone: (617) 253-1892. Fax: (617) 258-8150.


### Notes

The authors declare no competing financial interest.

## ■ ACKNOWLEDGMENTS

This work was supported by Grant CHE0907905 from the National Science Foundation.

## ■ REFERENCES


(1) (a) Calabrese, V.; Mancuso, C.; Calvani, M.; Rizzarelli, E.; Butterfield, D. A.; Stella, A. M. G. *Nat. Rev. Neurosci.* **2007**, *8*, 766. (b) Bronte, V.; Zanovello, P. *Nat. Rev. Immunol.* **2005**, *5*, 641. (c) Furchgott, R. F.; Vanhoutte, P. M. *FASEB J.* **1989**, *3*, 2007. (d) Ignarro, L. J.; Buga, G. M.; Wood, K. S.; Byrns, R. E.; Chaudhuri, G. *Proc. Natl. Acad. Sci. U. S. A.* **1987**, *84*, 9265. (e) Rapoport, R. M.; Draznin, M. B.; Murad, F. *Nature (London)* **1983**, *306*, 174.

(2) (a) Tennyson, A. G.; Lippard, S. J. *Chem. Biol.* **2011**, *18*, 1211. (b) Bogdan, C. *Nat. Immunol.* **2001**, *2*, 907. (c) Isaac, J.; Tarapore, P.; Zhang, X.; Lam, Y.-W.; Ho, S.-M. *Biochemistry* **2012**, *51*, 9689.

(3) (a) Crack, J. C.; Green, J.; Hutchings, M. I.; Thomson, A. J.; Le Brun, N. E. *Antioxid. Redox Signaling* **2012**, *17*, 1215. (b) Saini, V.; Farhana, A.; Glasgow, J. N.; Steyn, A. J. C. *Curr. Opin. Chem. Biol.* **2012**, *16*, 45.

(4) (a) Drapier, J.-C. *Methods (San Diego)* **1997**, *11*, 319. (b) Styś, A.; Galy, B.; Starzyński, R. R.; Smuda, E.; Drapier, J.-C.; Lipiński, P.; Bouton, C. *J. Biol. Chem.* **2011**, *286*, 22846.

(5) (a) Crack, J. C.; Smith, L. J.; Stapleton, M. R.; Peck, J.; Watmough, N. J.; Buttner, M. J.; Buxton, R. S.; Green, J.; Oganesyan, V. S.; Thomson, A. J.; Le Brun, N. E. *J. Am. Chem. Soc.* **2010**, *133*, 1112. (b) Crack, J. C.; Stapleton, M. R.; Green, J.; Thomson, A. J.; Le Brun, N. E. *J. Biol. Chem.* **2013**, *288*, 11492. (c) Crack, J. C.; Green, J.; Thomson, A. J.; Le Brun, N. E. *Curr. Opin. Chem. Biol.* **2012**, *16*, 35.

(6) (a) Harrop, T. C.; Tonzetich, Z. J.; Reisner, E.; Lippard, S. J. *J. Am. Chem. Soc.* **2008**, *130*, 15602. (b) Tsou, C.-C.; Lin, Z.-S.; Lu, T.-T.; Liaw, W.-F. *J. Am. Chem. Soc.* **2008**, *130*, 17154.

(7) (a) Drapier, J. C.; Pellat, C.; Henry, Y. *J. Biol. Chem.* **1991**, *266*, 10162. (b) Kennedy, M. C.; Antholine, W. E.; Beinert, H. *J. Biol. Chem.* **1997**, *272*, 20340.

(8) Watmough, N. J.; Butland, G.; Cheesman, M. R.; Moir, J. W. B.; Richardson, D. J.; Spiro, S. *Biochim. Biophys. Acta, Bioenerg.* **1999**, *1411*, 456.

(9) (a) Tonzetich, Z. J.; Wang, H.; Mitra, D.; Tinberg, C. E.; Do, L. H.; Jenney, F. E., Jr.; Adams, M. W. W.; Cramer, S. P.; Lippard, S. J. *J. Am. Chem. Soc.* **2010**, *132*, 6914. (b) Tinberg, C. E.; Tonzetich, Z. J.; Wang, H.; Do, L. H.; Yoda, Y.; Cramer, S. P.; Lippard, S. J. *J. Am. Chem. Soc.* **2010**, *132*, 18168.

(10) Chen, T.-N.; Lo, F.-C.; Tsai, M.-L.; Shih, K.-N.; Chiang, M.-H.; Lee, G.-H.; Liaw, W.-F. *Inorg. Chim. Acta* **2006**, *359*, 2525.

(11) (a) Ciurli, S.; Carrie, M.; Weigel, J. A.; Carney, M. J.; Stack, T. D. P.; Papaefthymiou, G. C.; Holm, R. H. *J. Am. Chem. Soc.* **1990**, *112*, 2654. (b) Stack, T. D. P.; Holm, R. H. *J. Am. Chem. Soc.* **1988**, *110*, 2484. (c) Zhou, C.; Holm, R. H. *Inorg. Chem.* **1997**, *36*, 4066.

(12) Lorković, I. M.; Ford, P. C. *Inorg. Chem.* **2000**, *39*, 632.

(13) Stack, T. D. P.; Holm, R. H. *J. Am. Chem. Soc.* **1987**, *109*, 2546.

(14) Kent, T. A. *WMOSS v. 2.5: Mössbauer Spectral Analysis Software*; WEB Research Co.: Minneapolis, MN, 1998.

(15) *APEX2 v2009*; Bruker AXS: Madison, WI, 2009.

(16) Sheldrick, G. M. *SADABS: Area-Detector Absorption Correction*; University of Göttingen: Göttingen, Germany, 2008.

(17) (a) Sheldrick, G. *Acta Crystallogr., Sect. A: Found. Crystallogr.* **2008**, *64*, 112. (b) Sheldrick, G. M. *SHELXTL97: Program for Refinement of Crystal Structures*; University of Göttingen: Göttingen, Germany, 1997.

(18) Dolomanov, O. V.; Bourhis, L. J.; Gildea, R. J.; Howard, J. A. K.; Puschmann, H. *J. Appl. Crystallogr.* **2009**, *42*, 339.

(19) Weigel, J. A.; Holm, R. H. *J. Am. Chem. Soc.* **1991**, *113*, 4184.

(20) Rao, P. V.; Holm, R. H. *Chem. Rev.* **2004**, *104*, 527.

(21) D'Addario, S.; Demartin, F.; Grossi, L.; Iapalucci, M. C.; Laschi, F.; Longoni, G.; Zanello, P. *Inorg. Chem.* **1993**, *32*, 1153.

(22) Chu, C. T.-W.; Lo, F. Y.-K.; Dahl, L. F. *J. Am. Chem. Soc.* **1982**, *104*, 3409.

(23) Chu, C. T.-W.; Dahl, L. F. *Inorg. Chem.* **1977**, *16*, 3245.

(24) Butler, A. R.; Glidewell, C.; Li, M.-H. *Adv. Inorg. Chem.* **1988**, *32*, 335.

(25) Hopmann, K. H.; Ghosh, A.; Noodleman, L. *Inorg. Chem.* **2009**, *48*, 9155.

(26) Sedney, D.; Reiff, W. M. *Inorg. Chim. Acta* **1979**, *34*, 231.

(27) Sarte, B.; Stanford, J.; LaPrice, W. J.; Uhrich, D. L.; Lockhart, T. E.; Gelerinter, E.; Duffy, N. V. *Inorg. Chem.* **1978**, *17*, 3361.

(28) (a) Foster, M. W.; Cowan, J. A. *J. Am. Chem. Soc.* **1999**, *121*, 4093. (b) Duan, X.; Yang, J.; Ren, B.; Tan, G.; Ding, H. *Biochem. J.* **2009**, *417*, 783.
(29) Tonzetich, Z. J.; McQuade, L. E.; Lippard, S. J. *Inorg. Chem.* **2010**, *49*, 6338.
(30) Kalyvas, H.; Coucouvanis, D. *Inorg. Chem.* **2006**, *45*, 8462.